Distinguishing reactive isomers in premixed laminar low-pressure flames by using PEPICO spectroscopy

T. Bierkandt[*,1], P. Hemberger[2], P. Oßwald[3], M. Köhler[3], E. Akyildiz[1], A. Bodi[2], T. Gerber[2], T. Kasper[1]

[1]Institute for Combustion and Gas Dynamics, University of Duisburg-Essen, Germany
[2]Molecular Dynamics Group, Paul Scherrer Institut, Switzerland
[3]Institute of Combustion Technology, German Aerospace Center, Germany

Abstract

Fuel-rich flames (ϕ=1.8) of ethanol, 1,3-butadiene, and m-xylene were investigated at low-pressure (40-50 mbar) with special emphasis on the identification of reactive radicals, especially fuel radicals (C_2H_5O, C_4H_5, and C_8H_9) and some other important isomers (e.g. CH_3O, C_8H_8, $C_{11}H_{10}$). Measurements were performed at the Swiss Light Source (SLS), where single-photon ionization with VUV radiation offers a soft ionization technique for the sampled species. Isomer-selective detection is achieved by imaging photoelectron photoion coincidence (iPEPICO) techniques which comprises time-of-flight mass spectrometry and photoelectron spectroscopy. Measured photoionization efficiency curves and threshold photoelectron spectra are compared with reference spectra from the literature or calculated Franck-Condon simulations. Quantification of the major species as well as several intermediate species for all flames yields data sets for model validation.

Introduction

Although the amount of alternative energy carriers is increasing, currently more than 80% of the world energy consumption is covered by fossil fuels (oil, natural gas, and coal) and fossil fuels will also be the most important primary energy carrier in the next years [1]. So, a further understanding in combustion processes is still necessary to control the emissions of pollutants like polycyclic aromatic hydrocarbons (PAHs), soot, oxygenates, and NO_x. Especially, the investigation of reactive combustion intermediates is important because they influence pollutant formation.

The use of biofuels can reduce the formation of aromatic compounds and soot and ethanol is one of widely used biofuels worldwide. Ethanol was studied in detail in previous work under different conditions as single fuel [2,3] and additive [4,5], respectively. Particularly, the ability for soot reduction is often shown. 1,3-Butadiene is suited to investigate the formation of benzene as the first aromatic ring which is important for the formation of all further PAHs and therefore for soot [6]. The formation of the propargyl radical plays here a key role. It is an important soot precursor because of the recombination reaction ($C_3H_3 + C_3H_3 \rightleftharpoons C_6H_6$) to benzene. Laminar flames of xylenes [7,8] were also studied before but less extensive than ethanol.

An established technique to identify and quantify combustion species, especially reactive radicals, in premixed laminar low-pressure flames is molecular-beam mass spectrometry (MBMS). It can be combined with different ionization techniques, e.g. electron ionization, single photon ionization, and REMPI (resonance enhanced multiphoton ionization). MBMS measurements typically result in speciation data for the validation of chemical kinetic reaction mechanisms [9]. One of the main experimental challenges is the transfer of the gas sample from the flame into the mass analyzer without changing the gas composition. It is typically accomplished through quenching reactions by either a rapid reduction in pressure or by dilution with an inert gas. Another challenge is the discrimination between isomers. In principle, this can be done by comparison of measured photoionization efficiency (PIE) curves with already known ionization energies or calculated values of possible species. This procedure works well for the isomer with the lowest ionization energy. The assignment of higher thresholds can become difficult because changes in the slopes of the ionization efficiency curve do not necessarily correlate with ionization thresholds of other isomers. Photoelectron photoion coincidence (PEPICO) spectroscopy, which detects the electrons that are produced in the ionization process in coincidence with the ions, enables the measurement of mass-selected threshold photoelectron spectra (ms-TPES). These spectra can help to facilitate species detection because vibrational transitions from the neutral to specific ionic states can be observed yielding a fingerprint of the molecule [10].

Experiments

We have investigated fuel-rich flames of ethanol, 1,3-butadiene, and m-xylene at low-pressure with a stoichiometry of 1.8 for all three flames. The exact flame conditions can be found in Table 1. Conditions for 1,3-butadiene and m-xylene are the same as in the work of Hansen et al. [6] and Li et al. [7], respectively.

All measurements are performed at the Swiss Light Source of the Paul Scherrer Institute in Villigen, Switzerland where photoionization (PI) is achieved by tunable vacuum ultraviolet synchrotron radiation.

Liquid fuels are continuously evaporated in a heated vaporizer and the steam is then introduced with the argon flow as carrier gas into the mixing chamber of the

[*] Corresponding author: thomas.bierkandt@uni-due.de

burner where it is mixed with the oxidant. All the gas flows are adjusted by calibrated mass flow controllers (MKS Instruments) and the flames are stabilized on a McKenna-type burner with a 6-cm-diameter water-cooled sintered plate.

Table 1. Flame conditions.

	ethanol	butadiene	m-xylene
Φ	1.8	1.8	1.8
p [mbar]	50	40	40
v_{300K} [cm/s]	52.5	71.1	35.0
x(Ar)	0.250	0.693	0.500
x(O2)	0.470	0.231	0.427
x(fuel)	0.280	0.076	0.073

Sample is draw directly from the flame at different burner positions by a quartz nozzle (mounted on a water-cooled flange). The gas sample expands through the 400-µm orifice in the sharp tip of the nozzle to the intermediate vacuum chamber with a pressure of 10^{-4} mbar. Through a second stage of expansion to 10^{-6} mbar via a skimmer from Beam Dynamics with an aperture of 2 mm, the center of the molecular beam reaches the ionization chamber where it intersects with the photon beam. A gas filter (filled with Neon, Krypton or Argon) or a MgF_2 window was used to eliminate second order radiation in a range of 5-21 eV.

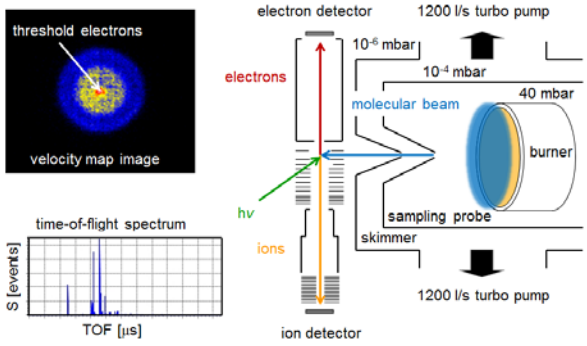

Fig. 1. Sketch of the molecular beam formation and detection schemes employed in the PEPICO experiment at the SLS.

Mass separation is achieved by a time-of-flight mass spectrometer (ToF-MS) with a mass resolution of $m/\Delta m \approx 300$. Electrons produced in the ionization process are velocity map imaged (Fig. 1). Each electron can be assigned to a single ionization event, enabling the measurement of mass-selected threshold photoelectron spectra. Figure 2 shows a schematic picture of the PI-MBMS system and more details about this systemcan be found in [10-12].

Data reduction

Procedures for the evaluation of species mole fractions follow the specifications from [10] and [13]. Flame species are identified by their ionization energies, PIE and TPE spectra. This is even possible for isomers. The spectra of the energy and burner scans are integrated for all masses. Afterwards the integrated signal intensity is normalized to the averaging time. Mass discrimination effects could not be observed so that a correction is not necessary. Finally, the integrated signal intensities are corrected by an instrument factor which takes into account the overall detection efficiency between the measurements with different settings.

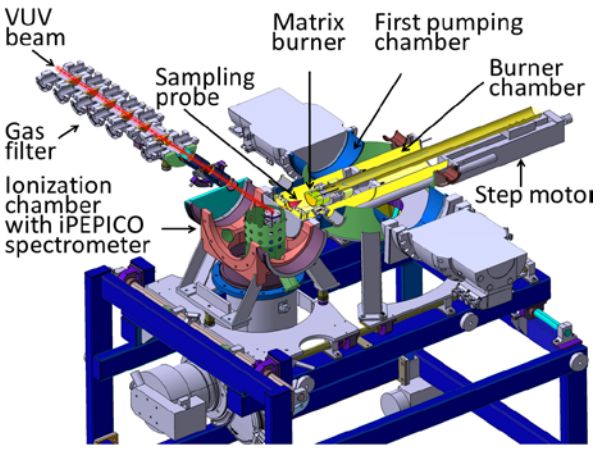

Fig. 2. Technical drawing of the PI-MBMS system at the SLS.

Now the major species (H_2, H_2O, C_2H_2, CO, O_2, Ar, CO_2, and the fuel) mole fractions can be calculated from the signal intensities of the high energy scans (16 or 14.35 eV), the flame conditions and the element balance for C, O and H. Furthermore, it is necessary to know the photoionization cross section ratio between CO to CO_2 or to calculate them from cold gas measurements. If required, a correction for ^{13}C, ^{18}O and fragmentation patterns is performed. The mole fractions of all other minority species are now available from argon as reference species. It is estimated from previous measurements that the error of the major species mole fractions is not greater than 20%. For species with unmeasured photoionization cross section, the accuracy may be worse. To obtain the threshold photoelectron spectra the central part of the electron image (threshold electrons) is selected and corrected for hot electron contamination.

Results and Discussion

The temperature profiles were determined from the temperature dependence of the sampling rate through the quartz nozzle and were used for the chemical kinetic modeling. We used the current models of E. Ranzi et al. [14] to simulate the experimental data. Figure 3 shows the experimental mole fraction profiles of the major species in the ethanol and m-xylene flame in comparison to the modeling results. In general, all calculated major mole fractions are in good agreement with the experimental values. There are only some discrepancies for the fuel-rich ethanol flame close to the burner surface. Oxygen und the fuel are lower than the model predicts while CO and CO_2 are higher.

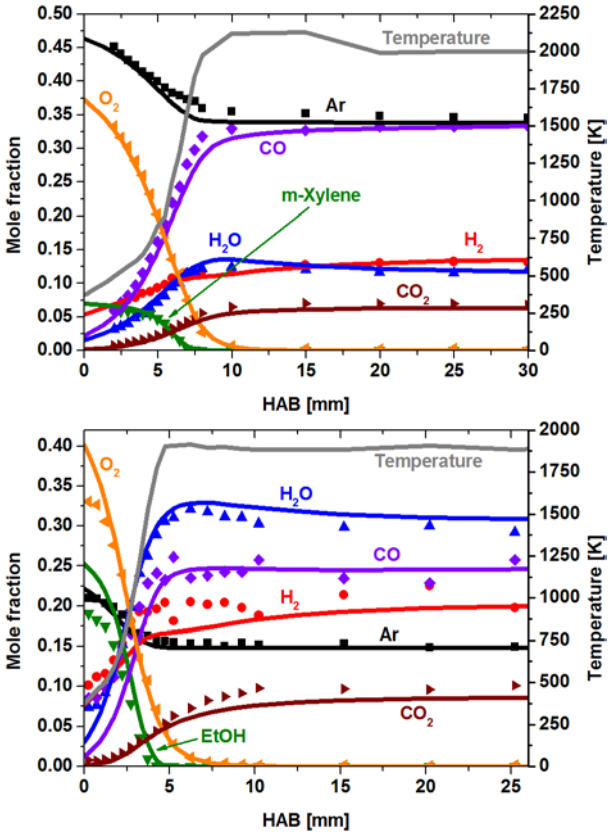

Fig. 3. Temperature profiles and mole fraction profiles of the major species in the fuel-rich m-xylene (top) and ethanol (bottom) flames. Symbols: experiment, lines: modeling.

For many stable intermediate species with well-known cross section the calculated mole fractions are reproduced quite well by the used model. This is shown in Fig. 4 where some experimental mole fractions of the fuel-rich m-xylene flame are compared to the modeling results.

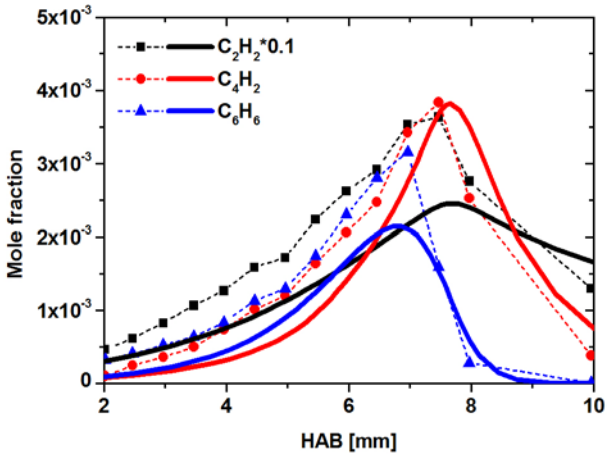

Fig. 4. Mole fraction profiles of acetylene, diacetylene, and benzene in the rich m-xylene flame. Symbols: experiment, lines: modeling.

The fuel radicals are formed by abstraction of a hydrogen atom and in all three flames different radical isomers can be detected. Information about the branching ratio is very useful for kinetic modeling for this first step of fuel destruction.

Ethanol flame

In the ethanol flame three possible fuel radicals (1-hydroxyethyl, 2-hydroxyethyl and ethoxy radical) can be formed by H-abstraction. The carbon-hydrogen bonds on the hydroxyl substituted carbon atom are weaker than the other hydrogen bonds in the ethanol molecule. Therefore, the 1-hydroxyethyl (CH_3CHOH) radical which is formed by H-abstraction from the α-site [3] by reaction of ethanol with mainly OH and H radicals is the most prevalent. The obtained PIE curve for m/z=45 is shown in Fig. 5.

The ionization energy of the 2-hydroxyethyl (CH_2CH_2OH) radical is unknown but it could be close to the 1-hydroxyethyl radical. Since the secondary radical is more stable and the ethoxy (CH_3CH_2O) radical is the least stable isomer [15], the curve is compared to the 1-hydroxyrthyl-PES of Dyke et al. [16]. Unfortunately, the concentration in our measurements is very low so that the TPE spectrum is too noisy to get sharp peaks for the adiabatic and the vertical ionization energies even with long averaging times but the onset in the PIE spectrum can be assigned to the ionization energy of 1-hydroxyethyl of 6.64 eV from [16].

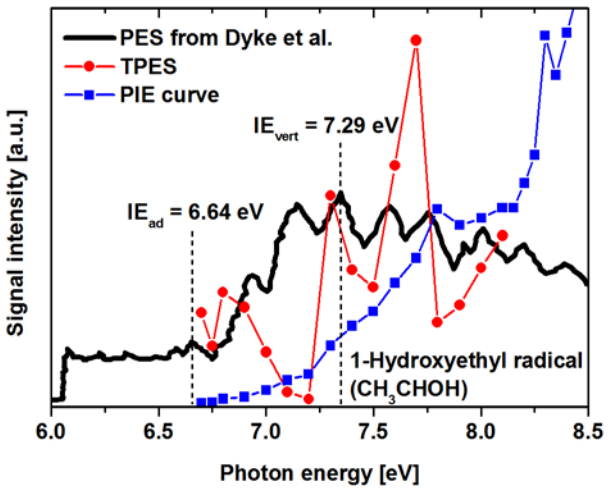

Fig. 5. Comparison of measured TPE spectrum of m/z=45 in fuel-rich ethanol flame to the photoelectron spectra of 1-hydroxyethyl radical from [16] and measured PIE curve.

Because of hyperconjugation the ionization energies of the hydroxymethyl (7.56 eV) and 1-hydroxyethyl (6.64 eV) radicals are rather different [17]. Hydroxymethyl (CH_2OH) is an important intermediate species for the formation of formaldehyde (CH_2O) and can be clearly identified in the fuel-rich ethanol flame by comparison of the experimental PIE spectrum to the simulated spectrum (Fig. 6). Another possible isomer is the methoxy radical but its ionization energy is high (10.72 eV) so that a distinction between these two isomers is easy. A quantitative separation between these radicals was possible (Fig. 7) but there is a huge deviation in the experimental and simulated mole

fraction of the hydroxymethyl radical. For the interpretation of this result, it must be considered that the mole fraction of the hydroxymethyl was calculated from a burner scan at 8.95 eV. This energy is distinctly higher than the ionization threshold so that a correction is needed. Furthermore, the cross section is unknown and estimated values were used in this case for the calculations. By contrast, calculated and simulated mole fractions of the methoxy radical agree very well.

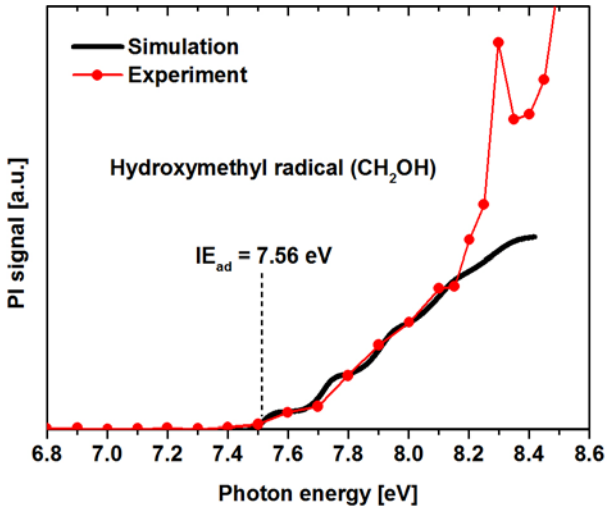

Fig. 6. Simulated PIE spectrum of the hydroxymethyl radical and the experimental PIE curve of m/z=31 measured in fuel-rich ethanol flame.

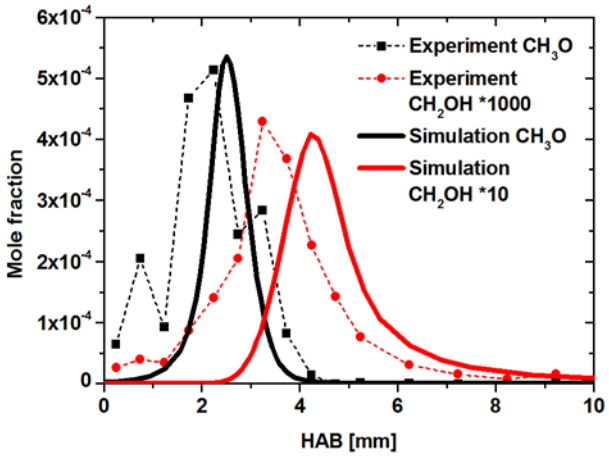

Fig. 7. Comparison of experimental (symbols) and simulated (lines) mole fractions of the hydroxymethyl (CH_2OH) and methoxy (CH_3O) radicals in the ethanol flame.

1,3-Butadiene flame

Benzene formation in 1,3-butadiene flames is directly influenced by the concentration of propargyl radicals due to the recombination reaction ($C_3H_3 + C_3H_3 \rightleftharpoons C_6H_6$) and also the reaction of *i*-C_4H_5 with acetylene to benzene is very important [6]. The *i*-C_4H_5 radical (CH_2CHCCH_2) is one possible fuel radical which is formed by hydrogen abstraction of 1,3-butadiene. Figure 8 shows a comparison of our measured PIE curve for m/z=53 at 3.5 mm above the burner to a Franck-Condon simulation for the photoionization of *i*-C_4H_5 by Hansen et al. [18] which confirms the presence of this radical in the 1,3-butadiene flame. The observed onset at 7.54 eV fits perfectly to the calculated value of 7.55 eV in [18]. In contrast, the *n*-C_4H_5 radical ($CHCHCHCH_2$) plays only a minor role for benzene formation because of its low concentration in comparison to the resonantly stabilized *i*-isomer. The second onset at about 7.95 eV can be assigned to the CH_3CHCCH and CH_3CCCH_2 radicals. Both species have similar simulated PIE spectra [18] so that a distinction is not possible.

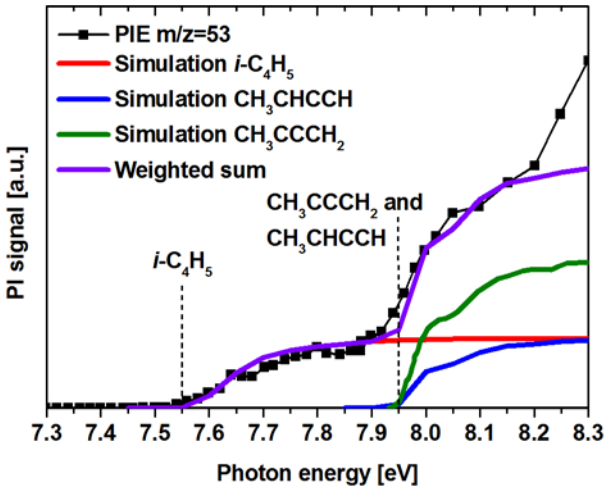

Fig. 8. PIE curve of the m/z=53 signal (C_4H_5) obtained from the reaction zone of a fuel-rich 1,3-butadiene flame. Signals are compared to the adiabatic ionization energies and Franck-Condon simulations of *i*-C_4H_5, CH_3CHCCH, and CH_3CCCH_2 radicals from [18].

Butenyl radicals (C_4H_7) occur by hydrogen addition reactions to 1,3-butadiene and are intermediates for the formation of methyl radicals and C_3H_4 [19]. Other C_4H_7 radicals could be the cyclobutyl and 2-methylallyl radicals. Heats of formations are similar for the 1-buten-3-yl and 2-methylally radicals while the values for the cyclobutyl and but-3-en-1-yl radicals are significantly higher [20]. Therefore, it is expected that the 1-buten-3-yl radical dominates in 1,3-butadiene flames because in contrast to the 2-methylallyl radical it does not need to undergo a isomerization. This can be confirmed when the measured TPE spectrum for m/z=55 is compared to the photoelectron spectra from [20] and is shown in Fig. 9. Because the vertical ionization energy for the cyclobutyl radical is only 0.01 eV smaller than for the 1-buten-2-yl radical and there is also a small peak at the adiabatic ionization energy, the existence cannot be completely excluded. However, the concentration should be much lower. The but-3-en-1-yl radical could be there in the rich 1,3-butadiene flame but cannot be confirmed by the TPES because the step width is too wide to see a peak in the region of the vertical ionization energy of 8.47 eV and is therefore not shown up to this value but there is a small change in the slope of the PIE curve at the adiabatic ionization energy of 8.04 eV.

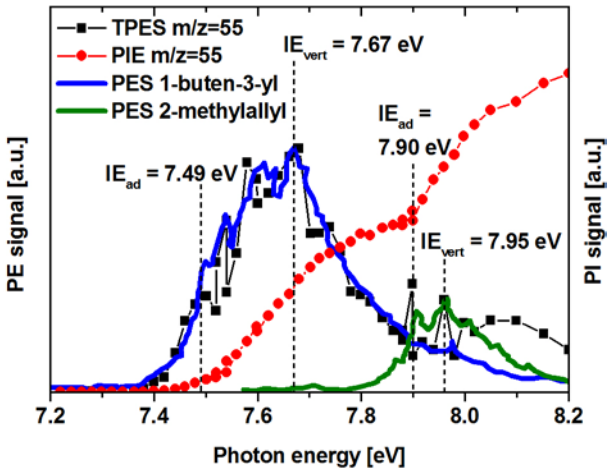

Fig. 9. PIE curve and TPES of the m/z=55 signal (C_4H_7) obtained from the reaction zone of a fuel-rich 1,3-butadiene flame. Signals are compared to the adiabatic and vertical ionization energies and PES of 1-buten-3-yl and 2-methylallyl radical from [19], respectively.

m-Xylene flame

For m-xylene we expect the m-xylyl radical (C_8H_9) as the dominant fuel radical. This radical can be clearly identified from the measured TPES in the reaction zone of the rich m-xylene flame. Figure 10 shows the comparison of the experimental and calculated TPES from [21]. There is a sharp peak at the adiabatic ionization energy and two other characteristic peaks from transitions. The small peak at 7.055 eV seems to be a hot band. The presence of the other xylyl radicals (m-xylyl and p-xylyl) can be excluded. This observation matches the investigations of Li et al. [7] where in the fuel-rich xylene flames only the corresponding xylyl radicals were detected. Hydrogen abstraction on the benzenoid ring instead of the methyl group does not occur or plays only a minor role so that the concentration of those radicals is under the detection limit.

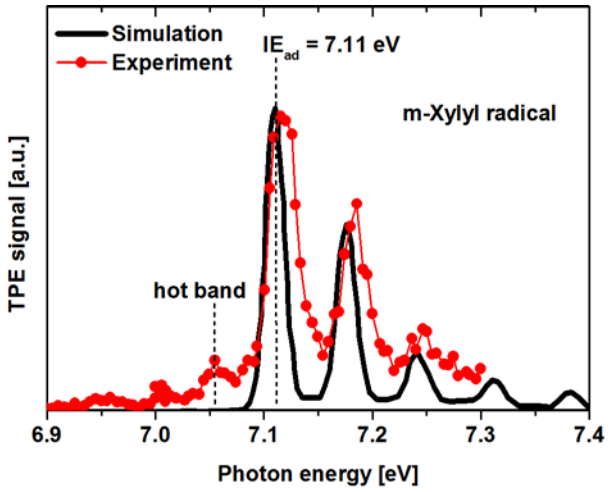

Fig. 10. TPE spectrum of m/z=105 measured in the rich m-xylene flame compared to a Franck-Condon simulation of the m-xylyl radical from [21].

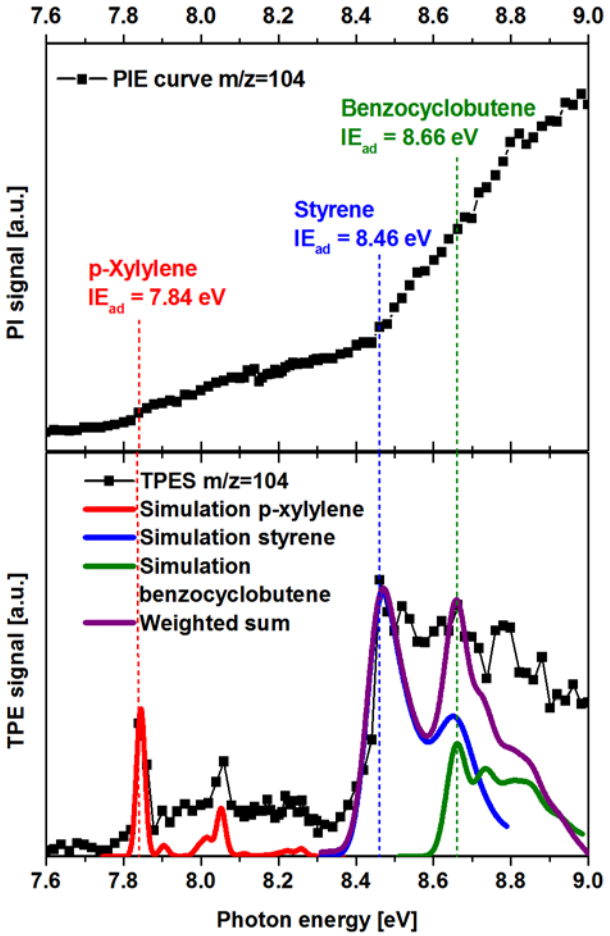

Fig. 11. Measured PIE curve (top) and TPE spectrum (bottom) of m/z=104 in the m-xylene flame and comparison to Franck-Condon simulation of p-xylylene, styrene, and benzocyclobutene.

A further decomposition of the m-xylyl radical leads to the formation of C_8H_8. Overall, three species can be identified by comparison of the measured TPES to Franck-Condon simulations for p-xylylene, styrene, and benzocyclobutene (Fig. 11). Here, we make similar observations as for the decomposition of the m-xylyl and o-xylyl radical measured in a SiC reactor at different temperatures in previous work [21,22] where at temperatures above 1100 K, as in the reaction zone of the laminar flame, the above-mentioned C_8H_8 species were also identified. m-Xylylene was not observed in our measurements or in [21-23] so that a rearrangement of the m-xylyl to the p-xylyl or the o-xylyl radical must take place to obtain the p-xylylene [22]. However, the p-xylyl or the o-xylyl radical could not be measured in the flame. Hemberger et al. [21] also showed that the o-xylyl radical forms benzocyclobutene via o-xylylene. The presence of the benzocyclobutene in our flame (Fig. 11) indicates that this reaction also occurs here, although the o-xylyl radical or o-xylylene could not be detected. Benzocyclobutene itself isomerizes to styrene [22,24]. On the basis of the C_8H_8 isomers the big advantage of PEPICO can be seen. In the PIE curve a change in the slope after the adiabatic ionization energy

of the benzocyclobutene cannot be seen but on the basis of the mass-selected threshold photoelectron spectrum this species can be identified because of the peak at the adiabatic ionization energy of 8.66 eV.

Conclusions

In this study reactive intermediate species were identified in fuel-rich flames of ethanol, 1,3-butadiene, and m-xylene by imaging photoelectron photoionization coincidence spectroscopy at the Swiss Light Source in Villigen, Switzerland. The PEPICO experiment allows the simultaneous identification of combustion species with photoionization efficiency spectra and threshold photoelectron spectra. TPES gives a fingerprint for each molecule so that the identification can be easier especially at low ionization energies. However, it must be considered that more measurement time is needed to take TPE spectra with good signal-to-noise ratios in comparison to the PIE spectra.

In principal, the main species profiles for all flames can be reproduced quite well by the simulation with the reaction mechanism of Ranzi et al. [14]. But the comparison of the fuel radicals shows large deviations in the absolute mole fractions and the positions of profile maxima. This observation illustrates that on the one hand the quantification of these species is prone to large uncertainties because of the lack of photoionization cross sections. On the other hand, the models have not been tested against speciation data of these important intermediates before due to the difficulties in the experimental detection. The new instrument at the SLS provides access to these species for the first time and provides in addition superior species identification by the use of distinctive mass-selected threshold photoelectron spectra.

Acknowledgments

All experiments were carried out at the VUV beamline at the Swiss Light Source of the Paul Scherrer Institute. T.B., E.A., and T.K. are grateful for financial support from the Ministry of Innovation, Science and Research of the German state of North Rhine-Westphalia. Funding by the Helmholtz Associaction is acknowledged by P.O. and M.K. P.H., A.B., and T.G. acknowledge funding by the Swiss Federal Office for Energy under BFE Contract No. 101969/152433.

References

[1] International Energy Agency, World Energy Outlook, 2012.
[2] T.S. Kasper, P. Oßwald, M. Kamphus, K. Kohse-Höinghaus, Combust. Flame 150 (2007) 220-231.
[3] L.S. Tran, P.A. Glaude, R. Fournet, F. Battin-Leclerc, Energy Fuels 27 (2013) 2226-2245.
[4] V. Dias, H. Mbuyi Katshiatshia, H. Jeanmart, Combust. Flame 161 (2014) 2297-2304.
[5] T. Bierkandt, T. Kasper, E. Akyildiz, A. Lucassen, P. Oßwald, M. Köhler, P. Hemberger, Proc. Combust. Inst. 35 (2015) 803-811.
[6] N. Hansen, J.A. Miller, T. Kasper, K. Kohse-Höinghaus, P.R. Westmoreland, J. Wang, T.A. Cool, Proc. Combust. Inst. 32 (2009) 623-630.
[7] Y. Li, L. Zhang, T. Yuan, K. Zhang, J. Yang, B. Yang, F. Qi, C.K. Law, Combust. Flame 157 (2010) 143-154.
[8] L. Zhao, Z. Cheng, L. Ye, F. Zhang, L. Zhang, F. Qi, Y. Li, Proc. Combust. Inst. 35 (2015) 1745-1752.
[9] N. Hansen, T.A. Cool, P.R. Westmoreland, K. Kohse-Höinghaus, Prog. Energy Combust. Sci. 35 (2009) 168-191.
[10] P. Oßwald, P. Hemberger, T. Bierkandt, E. Akyildiz, M. Köhler, A. Bodi, T. Gerber, T. Kasper, Rev. Sci. Instrum. 85 (2014) 025101.
[11] A. Bodi, P. Hemberger, T. Gerber, B. Sztáray, Rev. Sci. Instrum. 83 (2012) 083105.
[12] A. Bodi, M. Johnson, T. Gerber, Z. Gengeliczki, B. Sztáray, T. Baer, Rev. Sci. Instrum. 80 (2009) 034101.
[13] T.A. Cool, K. Nakajima, C.A. Taatjes, A. Mcllroy, P.R. Westmoreland, M.E. Law, A. Morel, Proc. Combust. Inst. 30 (2005), 1681-1688.
[14] E. Ranzi, A. Frassoldati, R. Grana, A. Cuoci, T. Faravelli, A.P. Kelley, C.K. Law, Prog. Energy Combust. Sci. 38 (2012) 468-501.
[15] H. Choi, R.T. Bise, D.M. Neumark, J. Phys. Chem. A 104 (2000) 10112-10118.
[16] J.M. Dyke, A.P. Groves, E.P.F. Lee, M.H. Zamanpour Niavaran, J. Phys. Chem. A 101 (1997) 373-376.
[17] B. Karpichev, H. Reisler, A.I. Krylov, K. Diri, J. Phys. Chem. A 112 (2008) 9965-9969.
[18] N. Hansen, S.J. Klippenstein, C.A. Taatjes, J.A. Miller, J. Wang, T.A. Cool, B. Yang, R. Yang, L. Wei, C. Huang, J. Wang, F. Qi, M.E. Law, P.R. Westmoreland, J. Phys. Chem. A 110 (2006) 3670-3678.
[19] S. Granata, T. Faravelli, E. Ranzi, N. Olten, S. Senkan, Combust. Flame 131 (2002) 273-284.
[20] J.C. Schultz, F.A. Houle, J.L. Beauchamp, J. Am. Chem. Soc. 106 (1984) 7347-7351.
[21] P. Hemberger, A.J. Trevitt, T. Gerber, E. Ross, G. da Silva, J. Phys. Chem. A. 118 (2014) 3593-3604.
[22] P. Hemberger, A.J. Trevitt, E. Ross, G. da Silva, J. Phys. Chem. Lett. 4 (2013) 2546-2550.
[23] G. da Silva, E.E. Moore, J.W. Bozzelli, J. Phys. Chem. A 113 (2009) 10264-10278.
[24] O.L. Chapman, U.P.E. Tsou, J. Am. Chem. Soc. 106 (1984) 7974-7976.